Synergistic elimination of bacteria by phage and the immune system

Chung Yin (Joey) Leung* and Joshua S. Weitz†
School of Biological Sciences, Georgia Institute of Technology, Atlanta, Georgia 30332, USA and School of Physics, Georgia Institute of Technology, Atlanta, Georgia 30332, USA
(Dated: July 25, 2016)

Phage therapy has been viewed as a potential treatment for bacterial infections for over a century. Yet, the year 2016 marks the first phase I/II human trial of a phage therapeutic - to treat burn wound patients in Europe. The slow progress in realizing clinical therapeutics is matched by a similar dearth in principled understanding of phage therapy. Theoretical models and in vitro experiments find that combining phage and bacteria often leads to coexistence of both phage and bacteria or phage elimination altogether. Both outcomes stand in contrast to the stated goals of phage therapy. A potential resolution to the gap between models, experiments, and therapeutic use of phage is the hypothesis that the combined effect of phage and an immune system can synergistically eliminate bacterial pathogens. Here, we propose a phage therapy model that considers the nonlinear dynamics arising from interactions between bacteria, phage and the immune system. The model builds upon earlier efforts by incorporating a maximum capacity of the immune response and immune evasion by bacteria at high density. We analytically identify a synergistic regime in which phage and the immune response jointly contribute to the elimination of the target bacteria. Crucially, we find that in this synergistic regime, neither phage alone nor the immune system alone can eliminate the bacteria. We confirm these findings using numerical simulations in biologically plausible scenarios. We utilize our numerical simulations to explore the synergistic effect and its significance for guiding the use of phage therapy in clinically relevant applications.

Keywords: Bacteriophage, Phage therapy, Antibiotic resistance, Population dynamics, Mathematical model

I. INTRODUCTION

Phage therapy denotes the use of bacteriophage, or viruses that exclusively infect bacteria, as therapeutic agents to treat pathogenic bacteria infections. Phage therapy was applied in the 1920s and 1930s before the widespread use of antibiotics [1]. Early applications of phage therapy were plagued by a number of problems, caused in part by poor understanding of phage biology [2]. These issues range from the lack of proper testing of the host range of phage to inappropriate preparation methods of phage stocks that inactivate the phage. In addition, interest in phage therapy declined after the discovery and mass production of antibiotics. However, the rise of pervasive antibiotic resistance has led to a renewal of interest in using phage to treat bacterial infections [3].

The first international, single-blind clinical trial of phage therapy, Phagoburn, was launched in 2015 [4]. The trial is designed to target 220 burn patients whose wounds are infected by *Escherichia coli* or *Pseudomonas aeruginosa* [5, 6]. Other clinical trials are currently underway, including a phase I clinical trial by AmpliPhi Biosciences for treating infections of *Staphylococcus aureus* [6] and trials targeting respiratory tract infections such as pneumonia [6, 7]. Phage-based therapeutics have also been used for in vitro biocontrol of pathogenic or nuisance bacteria [8, 9], for example, in the reduction of populations of pathogens in produce [10], ready-to-eat foods [11] and meat [12].

* E-mail: cyleung2001@gatech.edu
† E-mail: jsweitz@gatech.edu

Phage therapy has a number of potential advantages over conventional drug therapy [13]. Phage can replicate inside bacterial cells and increase in number at the site of infection [2]. This self-amplification is in contrast to the fixed dose in conventional drug therapy [2, 14, 15]. A consequence of the self-amplification is that sufficiently high bacteria density is required for the proliferation of phage and the subsequent active control of bacteria [14, 16, 17]. Phage are also more specific than broad spectrum antibiotics. This specificity reduces negative impacts on the normal flora of the human host [18]. Some phage also have the ability to break down and clear biofilms which are resistant to antibiotics and recalcitrant to the host immune response [19–23]. Finally, innovations in genetic engineering provide a means to prototype and deploy combinations of phage targeted to individual infections [24, 25].

Despite reinvigorated interest in phage therapy, there remain many questions with respect to how, when, why, and even if phage therapy works. The elimination of a bacteria population by phage is not inevitable, even if phage can eliminate a targeted bacterial population given suitably chosen strains and initial conditions. Indeed, in-vitro experiments [26–29] and ecological models [30] of phage-bacteria systems predict broad regimes of coexistence among phage and bacteria populations. In many instances, co-coculturing of phage and bacteria together leads to the emergence of resistant host strains and the death of the phage population [29]. Such outcomes are not desirable from a therapeutic perspective.

The host immune response is also a key component of dynamics taking place in a bacterial infection. Experimental studies have revealed that host immune response

influences the efficacy of phage in clearing pathogenic bacteria in vivo [31–33]. Phage therapy was shown to be effective in treating bacterial infections in a normal mouse model but not in a neutropenic mouse model, suggesting a possible synergistic effect between phage and the immune response [31]. In addition, phage administration was demonstrated to increase immune activation in infected hosts, which may contribute to control of the bacterial infection [32]. However, a high level of induced inflammation from excessive phage dosage may be detrimental to immunocompromised hosts [33].

These results highlight the need to understand the role of the immune response in concert with phage therapy. Previous studies have focused on the combined, nonlinear interactions of bacteria, phage, and the immune system [34, 35]. In such a combined system, phage-bacteria interactions are presumed to operate concurrently with that of the immune response. The immune response eliminates bacteria and the intensity of the immune response is stimulated by the presence of bacteria. Standard models of bacteria-phage-immune system share a few simplifying assumptions [34, 35]. First, they assume that the immune system can grow in strength without bounds. Second, they assume that bacteria cannot evade the immune response. As a result, these models presuppose that bacteria will be eliminated by the immune system when acting alone given sufficient time post-infection. In this framework, the added benefit of phage is to accelerate the time at which the bacteria are eliminated.

Here, we extend earlier models to explore a clinically relevant regime in which bacteria elimination by the immune system is not inevitable, neither in the short- nor long-term. The dynamic model of phage therapy we propose includes two important biological features not previously explored [35]. First, we assume that the magnitude of the immune response is finite [36–38]. Second, we assume that bacterial pathogens utilize density-dependent mechanisms such as biofilm formation to evade the immune response [39–42]. We demonstrate that the inclusion of these two biological mechanisms are sufficient to give rise to a robust mechanism of effective phage therapy: synergistic elimination of a bacterial pathogen. This synergistic elimination is possible even when neither the immune response nor the phage can eliminate the bacterial pathogen, when acting alone. We discuss ways in which this synergistic mechanism can be leveraged in clinical settings.

II. RESULTS

A. A model of bacteria-phage-immune system

We propose a phage therapy model including interactions among bacteria, phage, and the immune system (see Fig. 1). In this model, the bacteria population reproduces and can be infected and lysed by phage. Phage particles can decay when outside of cells. The presence of bacteria activates the immune response which in turn kills the bacteria. This phage therapy model leverages core components proposed in Ref. [35]. In so doing, we include two additional features. First, we include a saturating immune response. The upper bound on the capacity of the immune response is set by a number of factors including the finite number of immune cells that can be supported [36] and limited efficiencies of the immune cells in clearing bacteria [37, 38]. In Fig. 1 this is represented as an inhibition of the immune activation when the immune response is high. Second, we include density-dependent immune evasion of bacteria. Many pathogenic strains of bacteria utilize population density-dependent strategies such as biofilm formation and production of virulence factors to evade the immune response [39–42]. The immune evasion results in suppression of the immune killing action at high bacteria density.

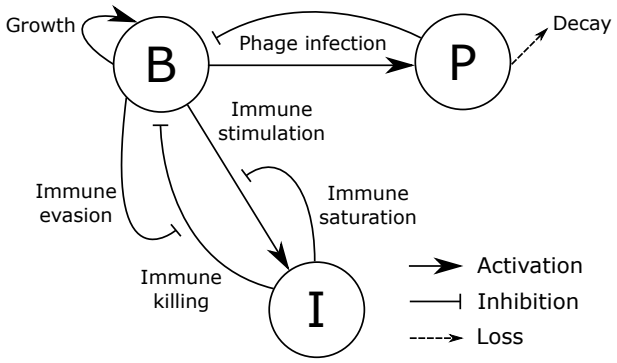

FIG. 1. Schematic diagram of a phage therapy model with immune saturation at maximum capacity and immune evasion by bacteria.

The interactions shown in Fig. 1 are modeled by the following set of differential equations that govern the temporal evolution of bacteria (B), phage (P), and the immune response (I):

$$\dot{B} = \overbrace{rB(1-\frac{B}{K_C})}^{\text{Growth}} - \overbrace{\phi BP}^{\text{Lysis}} - \overbrace{\frac{\epsilon IB}{1+B/K_D}}^{\text{Immune killing}}, \quad (1)$$

$$\dot{P} = \overbrace{\beta\phi BP}^{\text{Replication}} - \overbrace{\omega P}^{\text{Decay}}, \quad (2)$$

$$\dot{I} = \overbrace{\alpha I(1-\frac{I}{K_I})\frac{B}{B+K_N}}^{\text{Immune stimulation}}. \quad (3)$$

In this model, the maximal bacterial growth rate is r and the carrying capacity is K_C. Phage attach to and infect bacteria at an adsorption rate of ϕ, and release new viral particles with a burst size of β. The phage particles decay or get washed out at a rate of ω. We assume that killing of bacteria by the immune response follows a saturating mass action form with a maximum rate parameter ϵ. To model immune evasion by bacteria at high density, the immune killing rate is scaled by the denomi-

nator $(1+B/K_D)$. This saturation results in less efficient immune killing at high bacteria density with K_D being the bacteria density at which the host immune response is half as effective. The immune response is activated by the presence of bacteria with a maximum growth rate of α and saturates at a maximum capacity of K_I. Finally, K_N is the bacteria population density at which the immune response growth rate is half its maximum.

B. Fixed points of the system and possible infection outcomes

We analyze the fixed points of the system to understand possible outcomes of infection. The fixed points of the system can be categorized into three different classes (Table I). The first class has no bacteria but has a finite immune response, corresponding to a state in which the immune response has eliminated the bacteria. There is also no phage population as phage require bacteria to replicate and survive. In this class, the immune response can take on any value less than the maximum, K_I.

The second class of phage-free fixed points contain a nonzero population of bacteria. Here the immune response is insufficient to eliminate the bacteria even when it reaches its maximum level, $I^* = K_I$. The equilibrium bacteria density for this class of fixed points depends on the relative magnitude of the bacteria logistic growth rate $G(B) \equiv r(1-B/K_C)$ and the bacteria death rate caused by the maximum immune response $D(B) \equiv \frac{\epsilon K_I}{1+B/K_D}$. Figure 2 compares the bacterial growth rate with the maximum immune killing rate as functions of bacteria density. There is an unstable fixed point B_I^U and a stable fixed point B_I^S. B_I^U and B_I^S can be obtained by considering $G(B) = D(B)$ and solving the resulting quadratic equation, giving

$$B_I^U = \frac{K_C - K_D}{2} - \Delta \quad \text{and} \quad B_I^S = \frac{K_C - K_D}{2} + \Delta \tag{4}$$

where $\Delta \equiv \sqrt{(K_C+K_D)^2/4 - K_C K_D \epsilon K_I / r}$.

When the bacteria concentration is above B_I^U, the system will reach the stable fixed point $\{B^* = B_I^S, P^* = 0, I^* = K_I\}$ such that the bacteria population persists. This fixed point is reached when there is no phage and the immune response alone is insufficient in wiping out the bacteria. On the other hand, when the bacteria density is below B_I^U, the immune killing rate is greater than the bacteria growth rate so the immune response can eventually eliminate the bacteria and drive the system to a bacteria-free class I fixed point. Therefore B_I^U gives the threshold of bacteria density below which the maximum immune response can eliminate the bacteria.

The third class of fixed points exhibits coexistence of bacteria, phage and immune response. In this case, the phage persist by infecting and lysing the bacteria population, but the combined effect of phage predation and immune response is insufficient in bringing the bacteria population to zero. By Eqs. (1) and (2) the equilibrium bacteria and phage densities are given respectively by [30]

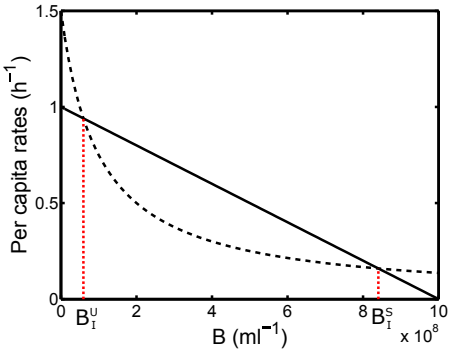

FIG. 2. Per capita rates of bacteria growth $G(B) \equiv r(1 - B/K_C)$ (solid line) and bacteria death $D(B) \equiv \frac{\epsilon K_I}{1+B/K_D}$ (dashed line) caused by the maximum immune response K_I as functions of bacteria density. The dotted vertical lines mark the positions of B_I^U and B_I^S.

$$B_{PI} \equiv \frac{\omega}{\beta\phi}, \tag{5}$$

$$P_{BI} \equiv \frac{1}{\phi}\left[r(1 - \frac{B_{PI}}{K_C}) - \frac{\epsilon K_I}{1 + B_{PI}/K_D}\right]. \tag{6}$$

The equilibrium level of bacteria in the coexistence state depends on the phage parameters. The equilibrium level is identical to the equilibrium density B_P when controlled by phage alone. For the coexistence fixed point to be feasible, the phage population density must be positive. A positive phage population occurs when the bacteria growth rate exceeds that of the immune killing rate given $B = B_P$. This condition is satisfied when $B_I^U < B_P < B_I^S$.

In summary, the bacteria can only be eliminated if the system reaches a class I bacteria-free fixed point. In a class II fixed point, the bacteria persists in the absence of phage. This can happen either when no phage is administered or when the phage administered cannot sustain its population and is eliminated. Finally, the combined killing action of phage and immune response is insufficient in eradicating the bacteria in a class III fixed point.

C. Demonstration of a possible synergistic effect between phage and immune response

Here we demonstrate that a synergistic effect can be realized in this phage therapy model. In Fig. 3, we compare the dynamics of bacteria, phage, and the immune response in three different cases. In the first case (Fig. 3(a)), the bacteria solely interact with phage. The bacteria and phage populations exhibit predator-prey oscillations. The oscillations are predicted to damp slowly so

Class	B^*	P^*	I^*	Outcome
I	0	0	$0 \leq I^* \leq K_I$	Bacteria elimination
II	$0 < B_I < K_C$	0	K_I	Bacteria persistence
III	$0 < B_{PI} < K_C$	$P_{BI} > 0$	K_I	Coexistence

TABLE I. The different classes of fixed points of the system and the corresponding infection outcome.

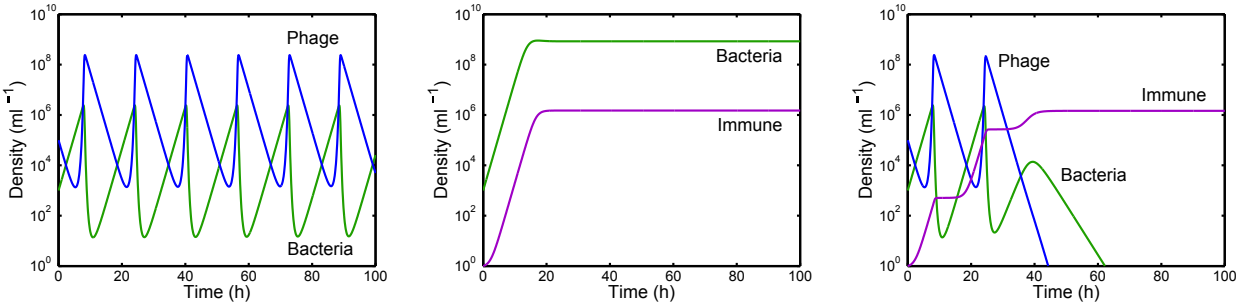

(a) (b) (c)

FIG. 3. Time series of bacteria density B (green curve), phage density P (blue curve) and immune response I (purple curve) in our model with (a) only bacteria and phage, (b) only bacteria and immune response, and (c) bacteria, phage and immune response combined.

that populations reach an equilibrium point (see Eqs. 5 – 6 with $\epsilon = 0$) [30]. In this case, the phage alone are unable to eliminate the bacteria. In the second case (Fig. 3(b)), the bacteria interact with the immune response in the absence of phage. Initially, there is rapid reproduction of the bacteria and the immune response grows as it is stimulated by the presence of bacteria. However, by the time it reaches its maximum value K_I, the bacteria has already reached a population that is sufficient to evade the maximum immune response K_I. The bacteria persist as the system reaches a class II fixed point. In this case immune response alone is insufficient in eliminating the bacteria. Finally, in Fig. 3(c) bacteria, phage and immune response are combined. In this case, predator-prey oscillations are observed initially, but as the immune response grows, the phage drive the system to a bacteria-free class I fixed point where the bacteria is eventually eliminated. The phage and immune response thus works in synergy to eliminate the bacteria. This synergistic effect is caused by a reduction of the bacteria population by phage below a level of B_I^U. At this level the bacteria are controlled by the immune response. With the elimination of the bacterial population, the phage are also eliminated.

D. Sufficient conditions for bacteria elimination through phage-immune synergy

Next, we simplify the system by applying a quasistatic approximation with the immune response treated as a constant. This simplification is justified given that bacteria and phage population are expected to change more rapidly than the immune response. We apply this approximation in the case when the immune response has reached its maximum K_I. This correspond to a scenario in which the immune response has not controlled a bacterial pathogen. Then phage are added as an additional therapeutic. In this event, the model equations in Eqs. (1) – (3) reduce to

$$\dot{B} = rB(1 - \frac{B}{K_C}) - \phi BP - \frac{\epsilon K_I B}{1 + B/K_D}\,, \tag{7}$$

$$\dot{P} = \beta\phi BP - \omega P\,. \tag{8}$$

In this approximation, we identify the synergistic effect to mean that phage drive the system from the class II fixed point $\{B^* = B_I^S, P^* = 0, I^* = K_I\}$ to the class I fixed point $\{B^* = 0, P^* = 0, I^* = K_I\}$. This transition corresponds to the scenario in which phage drive a system from one uncontrolled by the immune response to one in which both bacteria and phage are eliminated. This synergistic effect depends on the relative strength of phage and immune control of bacteria. The phage-controlled bacteria density is denoted as B_P. The bacterial density is B_I^S when the immune response alone cannot eliminate the bacteria. Synergistic elimination occurs when the phage drive the bacteria population from B_I^S to a value below B_I^U where the maximum immune response alone can eliminate the bacteria. This is guaranteed to happen if B_P is below B_I^U, i.e.

$$B_P = \frac{\omega}{\beta\phi} < B_I^U \tag{9}$$

We term this the sufficient condition for the synergistic elimination of bacteria.

In Figs. 4(a) and (b) we show the dynamics of the

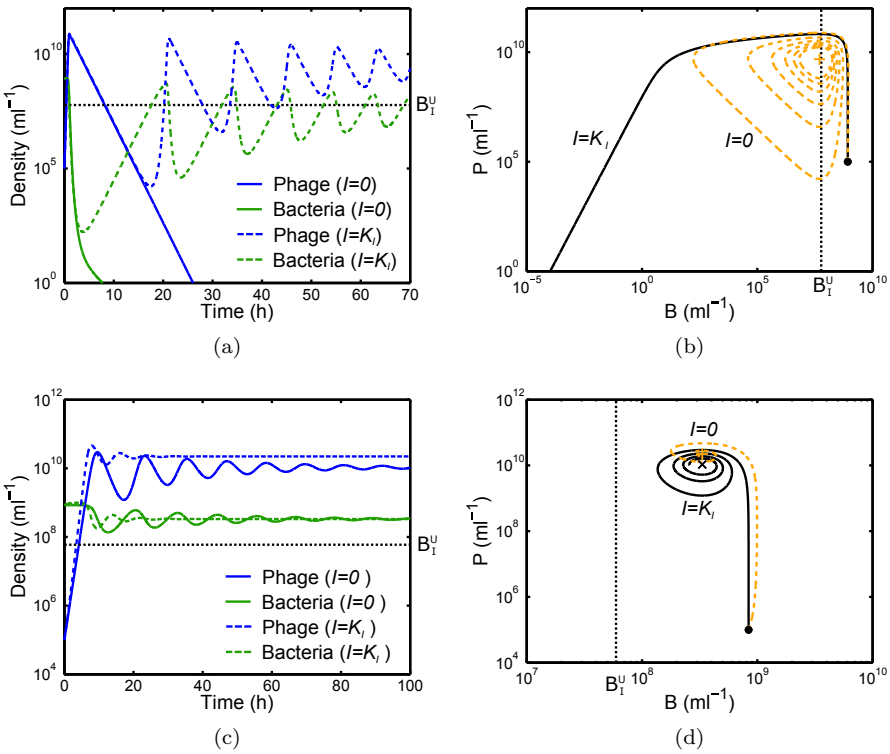

FIG. 4. Comparison of time series and phase portraits with and without immune response for two different adsorption rates. (a) Time series of bacteria (green curves) and phage densities (blue curves) with adsorption rate $\phi = 2.0 \times 10^{-10}$ ml h^{-1}. Solid lines are for the case of $I = K_I$ while dashed lines are for the case without immune response ($I = 0$). (b) shows the phase portrait for the time series in (a). Black solid line is the phase trajectory when $I = K_I$ while orange dashed line is the trajectory when $I = 0$. The initial conditions ($B_0 = B_I^S$, $P_0 = 10^5$ ml^{-1}) of the trajectory is marked by a filled circle and the fixed point for the case of $I = 0$ is denoted by a plus sign. (c) and (d) are the same as (a) and (b) but with an adsorption rate $\phi = 3.0 \times 10^{-11}$ ml h^{-1}. The coexistence fixed point $\{B^* = B_{PI}, P^* = P_{BI}, I^* = K_I\}$ is marked by a cross in (d).

system with an initial bacteria density $B_0 = B_I^S$ and administered phage with the adsorption rate ϕ chosen such that B_P is just below B_I^U. In the absence of immune response ($I = 0$), the bacteria and phage populations would converge to the fixed point $\{B^* = B_P, P^* = \frac{r}{\phi}(1 - \frac{B_P}{K_C})\}$ such that part of the trajectory corresponds to states with a bacteria level below B_I^U. For the set of parameters we consider, $B_I^U \approx 6.0 \times 10^7$ ml^{-1} and the sufficient condition is given by $\phi \gtrsim 1.7 \times 10^{-10}$ ml h^{-1}. As a result, the bacteria are eliminated given the maximum immune response $I = K_I$.

It is also important to consider the failure of the synergistic effect. In particular, when $B_I^U < B_P < B_I^S$, the coexistence steady state given by Eqs. (5) and (6) is feasible. In this event the phage drive the bacteria to the level B_P. The immune response effectively lowers the phage population at equilibrium (Figs. 4(c) and (d)) and there is no synergistic effect between phage and immune response. Finally, when $B_P > B_I^S$ the immune response would bring the bacteria density down to B_I^S which is insufficient to support the phage population. The phage decay at a faster rate than its replication and eventually die out while the bacteria infection persists.

E. Generalized conditions for bacteria elimination through phage-immune synergy

Here, we consider conditions in which the immune response alone cannot eliminate the bacteria. We initialize the system in a Class II fixed point. We then consider the effect of adding phage. In Fig. 5 we show simulation results for the steady state bacteria and phage density as functions of the phage decay rate ω and adsorption rate ϕ. When the phage decay at a slow rate and infects at a high rate which corresponds to a low B_P, it acts synergistically with the immune response to eliminate the bacteria. The thresholds $B_P = B_I^U$ and $B_P = B_I^S$ are compared to the simulation results and as expected when $B_P < B_I^U$ the synergistic effect is always able to exterminate the bacteria. In addition, when $B_P > B_I^S$ the bacteria persist but phage go extinct. The fixed point analysis predicted a feasible coexistence state of bacteria, phage and immune response when $B_I^U < B_P < B_I^S$, but in the simulation this is only observed for a subset of the region with B_P above an intermediate value B_I^M. This discrepancy can be explained by the stability of the coexistence state. The behavior of a dynamical system

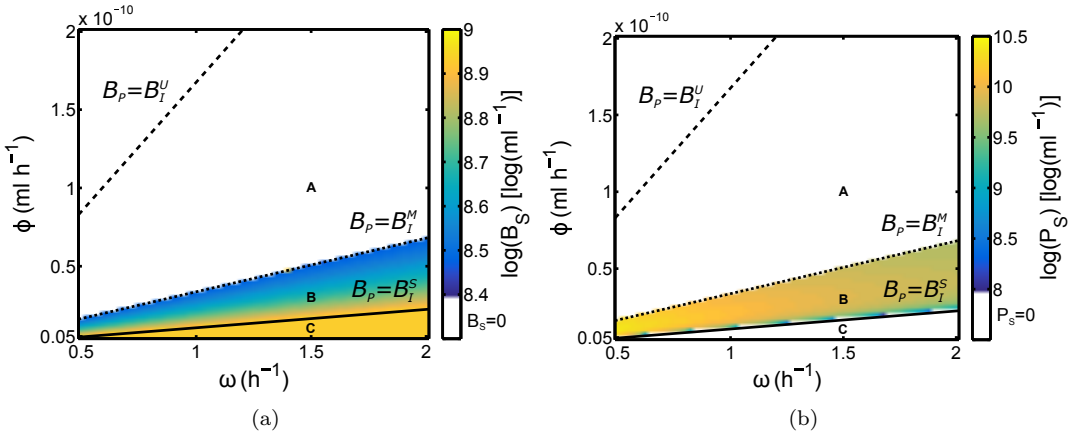

FIG. 5. Heat map showing the dependence of (a) log steady state bacteria density B_S and (b) log steady state phage density P_S on the phage decay rate ω and adsorption rate ϕ. The solid line is $B_P = B_I^S$, the dashed line is $B_P = B_I^U$ and the dotted line is $B_P = B_I^M$. The points labeled by A, B and C are sample points of the different regimes with time series shown in Figs. 6(a), (b) and (c) respectively. The initial conditions are given by $B_0 = B_I^S$, $P_0 = 10^5$ ml^{-1} and $I_0 = K_I$.

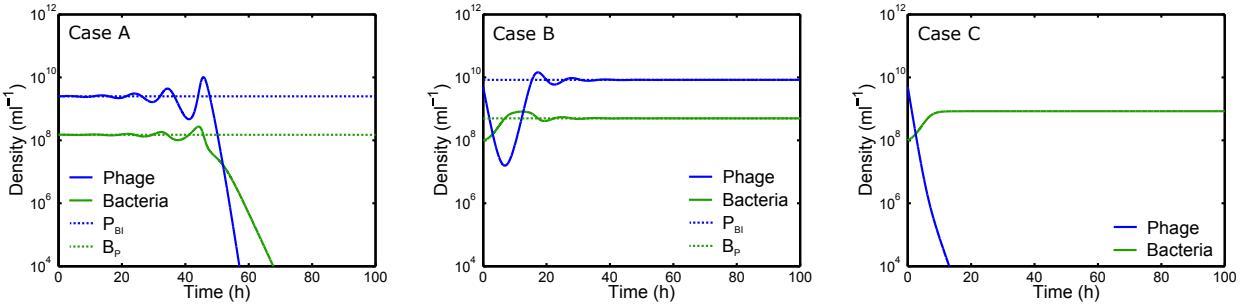

FIG. 6. Time series of bacteria (green curve) and phage densities (blue curve) at the three sample points A, B and C in Fig. 5: (a) $\phi = 10^{-10}$ ml h^{-1} ($B_I^U < B_P < B_I^M$), (b) $\phi = 3 \times 10^{-11}$ ml h^{-1} ($B_I^M < B_P < B_I^S$) and (c) $\phi = 10^{-11}$ ml h^{-1} ($B_P > B_I^S$). The phage decay rate $\omega = 1.5$ h^{-1} for all three cases. The simulations are initialized near the coexistence state marked by the dotted lines for (a) and (b). For (c) where the coexistence state is unfeasible, the initial conditions are $B_0 = 10^8$ ml^{-1} and $P_0 = 5 \times 10^9$ ml^{-1}.

near a fixed point can be analyzed by considering its Jacobian matrix evaluated at the fixed point [43].

In Appendix A we show that the condition for stability is:

$$B_P > K_D(\sqrt{\frac{\epsilon K_I K_C}{r K_D}} - 1) = B_I^M. \qquad (10)$$

In Fig. 6 we compare the time series of bacteria and phage densities at the three sample points A, B and C from Fig. 5. Case A satisfies $B_I^U < B_P < B_I^M$ while case B satisfies $B_I^M < B_P < B_I^S$. Although coexistence is feasible in both cases, it is unstable in case A and the escalating oscillations eventually cause extinction of the bacteria. We further verify that the stability condition in Eq. (10) gives the correct transition threshold $B_P = B_I^M$ from a coexistence state to bacteria extinction in Figure 5. For case C, $B_P > B_I^S$ and the coexistence state is unfeasible as it has negative phage density. In this case the phage is unable to sustain its population through replication, leading to premature phage extinction.

We summarize the results of the analysis in Table II. When $B_P < B_I^U$ the phage drive the bacteria population below a level that can be controlled by the immune response which leads to bacteria elimination by phage-immune synergy. When $B_I^U < B_P < B_I^S$, the phage can coexist with the bacteria in the presence of immune response, but when $B_P < B_I^M$ the coexistence is unstable and the oscillations can still drive the bacteria to extinction. Finally, when $B_P > B_I^S$ the phage become extinct rapidly as the bacteria persist at a level which cannot support phage growth. We conclude that the synergistic effect is enhanced when taking into account the stability of the coupled, nonlinear dynamical system. In Appendix B we show that the general results of the analysis and the enhanced synergy domain are robust to model formulations. We do so by extending the model to include an explicitly infected class of bacteria. In this scenario,

Condition	Effect of adding phage	Example
$B_P < B_I^U$	Phage-immune synergy (strict)	Fig. 4(a)
$B_I^U < B_P < B_I^M$	Phage-immune synergy (instability)	Fig. 6(a)
$B_I^M < B_P < B_I^S$	Stable coexistence	Fig. 6(b)
$B_P > B_I^S$	Phage extinction	Fig. 6(c)

TABLE II. Different regimes of the effect of phage therapy, the corresponding conditions and examples of time series in each regime.

we still find the same qualitative results as in the model where infection is modeled implicitly (see Fig. 8).

III. DISCUSSION

The science of phage therapy remains in its infancy despite renewed interest in translational and clinical applications. In particular, the interactions between bacteria, phage and the host immune response has yet to be fully characterized. Building on existing model of phage-bacteria-immune system [35], we developed a model of phage therapy that takes into account the finite capacity of the immune response and immune evasion of bacteria at high population densities. From our model, we identified a potential mechanism of phage therapy that relies on a synergistic effect between phage and the host immune response instead of through direct elimination of bacteria by phage. Our results are qualitatively consistent with the experimental observation that phage treatment is effective in protecting normal mice from bacterial infection but ineffective for neutropenic mice with a suppressed immune response [31].

The synergistic effect of phage therapy can be understood intuitively via the schematic in Fig. 7. In the initial phase of the infection, a small population of bacteria invade and reproduce within the human host. If the growth of the bacteria population is sufficiently fast compared to the activation of the immune response, the bacteria can reach a population large enough to utilize immune evasion strategies such as biofilm formation such that the immune response cannot eliminate the bacteria. The phage, on the other hand, have the ability to break down the biofilm [19–23] and continue to infect the bacteria. The resulting biofilm disruption and reduced bacteria population expose the bacteria to the action of the immune response which eventually eliminates the harmful bacteria. The phage population is eliminated as its target hosts are eliminated.

We have derived the conditions that predict the outcome of phage therapy in this model. The sufficient conditions for effective therapy depend on the relative strength of the phage and immune control of bacteria. Phage with a sufficiently high effectiveness acts synergistically with the immune response by lowering the bacteria population to a point where the immune response can then eliminate it. Phage with intermediate effectiveness can coexist with the immune response without clearing the bacteria infection. Phage with low effectiveness will become extinct prematurely.

The proposed model enables analytical solutions for the conditions under which the synergistic effect can eliminate the bacteria. These conditions facilitate the identification of general principles of the synergism. However, the simplification also results in certain limitations which will have to be addressed in future developments of the model. For example, our simulation results indicate that the time scale of the immune response is important in determining the outcome of infection and phage administration. The vertebrate immune system is composed of the innate and adaptive immune system. The innate immune response reacts faster than the adaptive system but the latter is more specific and generally more effective. Our model may be generalized to incorporate this added complexity by having an innate immune response I_i with a high immune activation rate α and a low capacity K_I in addition to an adaptive immune response I_a for which the converse is true. The effects of the existence of multiple time scales and immune response strengths on the outcome of phage therapy can then be investigated.

Another complication that may arise in the application of phage therapy is the development of phage resistance in bacteria. Bacteria employs a wide range of strategies to evade phage infection ranging from modification of surface receptors to degradation of exogenous genetic elements by mechanisms such as the CRISPR-Cas system [44]. Phage can also evolve counter-resistance and restore infectivity against resistant strains of bacteria, resulting in coevolution between the phage and bacteria [45–47]. Experiments have revealed that the coevolutionary dynamics can be categorized into at least two contrasting types: arms race dynamics where the bacteria becomes increasingly resistant while the phage become more infective, and fluctuating selection dynamics where there is no directional change in the bacteria resistance range and phage host range [48, 49]. Development of phage resistance in bacteria also alters the way they interact with the immune system and in many cases will lead to reduced virulence [50, 51]. The effects of the coevolutionary dynamics between bacteria, phage and immune response on the efficacy of phage therapy still remains unclear. Generalizing phage therapy models to include multiple evolved strains of bacteria and phage will be essential.

Finally, it has been recently suggested that phage may

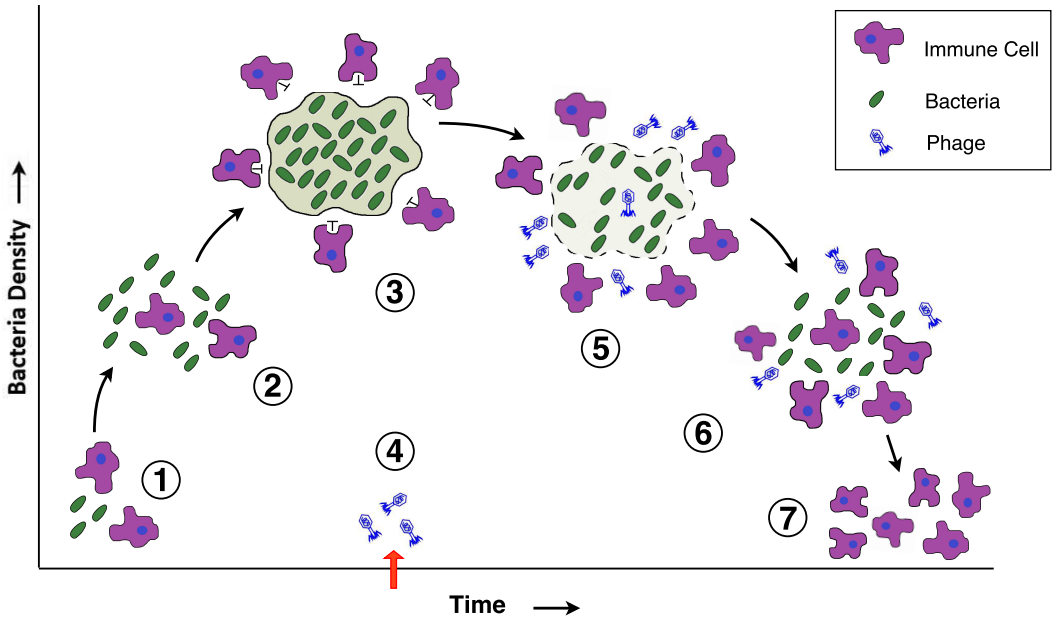

FIG. 7. Schematic of the mechanism of phage-immune synergy. Various stages of the infection and therapy: 1. Invasion of human host by bacteria, 2. Reproduction of bacteria, 3. Bacteria form a biofilm while immune response gets activated, 4. Administration of phage, 5. phage break down biofilm and reduce bacteria population, 6. Immune system gains access to bacteria, and 7. Elimination of bacteria by immune response while phage are eliminated due to the absence of bacteria.

be removed or degraded by the immune response of the host. Such removal may affect the clinical outcome of phage therapy [52]. This effect is assumed to be constant in our model and incorporated into the decay rate ω. However, the immune suppression of phage may increase as the bacteria activate the immune response. This can be modeled as a phage decay rate $\omega(I)$ that depends on the immune response. In such a case the outcome of phage administration is likely to depend on the relative strength between this direct immune inhibition of phage and the phage-immune synergistic effect.

How can we translate model findings into a therapeutic context? One finding of our model is that phage that are only partially effective in killing bacteria in vitro may still be effective in vivo due to the synergistic effect with the host immune response. Current screening of phage strains for phage therapy relies on in vitro killing [53, 54]. As a consequence, phage strains of therapeutic value may be overlooked. The synergistic effect observed in our model highlights the need to measure the interactions between bacteria, phage and components of the immune system both in vitro and in vivo. Such experiments complement prior studies involving phage and bacteria [27, 45, 55] and between bacteria and immune cells [56–58]. Information collected from such tripartite experiments would be important in understanding the effects of phage on microbes in the human body.

IV. METHODS

A. Model simulation

We simulate the model in Eqs. (1) – (3) and obtain the time series of the bacteria density, phage density and immune response intensity. The numerical integration is carried out using ode45 in MATLAB. A threshold for the population densities is implemented such that when the bacteria or phage densities fall below a set value $p_{th} = 1$ ml^{-1}, it is assumed to be extinct and the population density is set to 0. The steady state bacteria level B_S is estimated by running the simulation for a sufficiently long time ($T = 10000$ h) before averaging over a duration of $T_{av} = 1000$ h.

B. Parameter estimation

In Table III we show estimated values of the parameters in the model which are used in the simulations unless otherwise specified. The life history traits of the bacteria and phage are obtained from well-established empirical

Symbol and parameter	Value	Estimated from
r, growth rate of bacteria at low density	1 h^{-1}	A. baumannii and P. aeruginosa [37]
K_C, carrying capacity of bacteria	10^9 ml^{-1}	Bacterial load of P. aeruginosa in lung tissue of immunosuppressed mice [37]
β, burst size of phage	100	Phi1 phage in Salmonella [59] and within the range for coliphage [60]
ϕ, adsorption rate of phage	5×10^{-8} ml h^{-1}	Within the range for Lambda phage [61] and other coliphage [60]
ω, decay rate of phage	1 h^{-1}	Clearance of phage from blood of mice [52]
ϵ, killing rate parameter of immune response	10^{-6} ml h^{-1}	Neutrophils in vitro [56]
α, maximum growth rate of immune response	1 h^{-1}	Helper and cytotoxic T cells [62]
K_I, maximum capacity of immune response	1.5×10^6 ml^{-1}	Maximum neutrophil killing rate [37]
K_D, bacteria concentration at which immune response is half as effective	10^8 ml^{-1}	Reduction of antibiotics effectiveness at high bacteria density [63]
K_N, bacteria concentration when immune response growth rate is half its maximum	10^4 ml^{-1}	M. tuberculosis [64]
B_0, initial bacteria density	1000 ml^{-1}	Baseline inoculum of P. aeruginosa producing an infection [37]
P_0, initial phage dose	10^5 ml^{-1}	Phage dose for treating P. aeruginosa infection [65]
I_0, initial immune response	1 (ml^{-1})	Helper and cytotoxic T cells [62]

TABLE III. Estimated values of parameters in the model

values for common bacterial pathogens and their phage in the literature [37, 60, 61]. The decay rate ω of phage is estimated from measured clearance of phage from the blood of mice [52] and is higher than typical decay rates of phage in vitro [60]. The killing rate parameter of the immune response ϵ is estimated from in vitro measurements of neutrophils [56], which destroys pathogens by phagocytosis and is an essential part of the innate immune response. For the maximum growth rate of immune response α and initial immune response I_0, we use values typical of T cells proliferation [62]. Helper T cells play an important role in activating the immune system and one of its functions is to activate macrophage to increase its killing action and recruit more neutrophils to the infection site. We choose the maximum capacity K_I of the immune response such that the maximum bacteria killing rate is close to that measured for neutrophils [37]. Data is not available for the bacteria concentration K_D at which immune response is half as effective so we use the reduction of antibiotics effectiveness at high bacteria density as a surrogate with the latter having a significant effect at a bacteria concentration of around 10^8 ml^{-1} [63]. The bacteria density K_N at which immune growth rate is half its maximum is obtained from data of Mycobacterium tuberculosis [64]. Initial bacterial load and phage concentration are set by typical values of bacteria inoculum [37] and phage dose [65] for Pseudomonas aeruginosa infection.

Appendix A: Derivation of the stability condition for the coexistence state

Here we derive the condition for the coexistence state $\{B^* = B_P, P^* = P_{BI}\}$ to be stable. The type and stability of a fixed point can be characterized by the determinant $det(\mathbf{J})$ and trace $tr(\mathbf{J})$ of the Jacobian matrix $\mathbf{J}$ evaluated at the fixed point [43]. In particular, the stability of the system is determined by the signs of $det(\mathbf{J})$ and $tr(\mathbf{J})$.

Rewriting Eqs. (7) and (8) into $\dot{B} = f_B(B, P)$ and $\dot{P} = f_P(B, P)$ respectively, the Jacobian matrix of the system is defined as

$$\mathbf{J} \equiv \begin{bmatrix} \frac{\partial f_B}{\partial B} & \frac{\partial f_B}{\partial P} \\ \frac{\partial f_P}{\partial B} & \frac{\partial f_P}{\partial P} \end{bmatrix} \tag{A1}$$

We compute the Jacobian matrix by calculating the partial derivatives:

$$\frac{\partial f_B}{\partial B} = r(1 - \frac{B}{K_C}) - \frac{\epsilon K_I}{1 + B/K_D} - \phi P - \frac{rB}{K_C} + \frac{\epsilon K_I B}{K_D(1 + B/K_D)^2}, \tag{A2}$$

$$\frac{\partial f_B}{\partial P} = -\phi B, \tag{A3}$$

$$\frac{\partial f_P}{\partial B} = \beta\phi P, \tag{A4}$$

$$\frac{\partial f_P}{\partial P} = \beta\phi B - \omega. \tag{A5}$$

The Jacobian matrix of the system can therefore be writ-

ten as

$$\mathbf{J} = \begin{bmatrix} \frac{\partial f_B}{\partial B} & -\phi B \\ \beta\phi P & \beta\phi B - \omega \end{bmatrix}. \tag{A6}$$

At the coexistence state, the first line on the right hand side of Eq. (A2) vanishes as a result of Eq. (6). Together with $\beta\phi B_P - \omega = 0$, it yields the Jacobian matrix at coexistence

$$\mathbf{J} = \begin{bmatrix} -\frac{rB_P}{K_C} + \frac{\epsilon K_I B_P}{K_D(1+B_P/K_D)^2} & -\phi B_P \\ \beta\phi P_{BI} & 0 \end{bmatrix}. \tag{A7}$$

Equation (A7) gives the following determinant and trace:

$$det(\mathbf{J}) = \beta\phi^2 B_P P_{BI} = \omega\phi P_{BI} > 0\,, \tag{A8}$$

$$tr(\mathbf{J}) = \left[-\frac{r}{K_C} + \frac{\epsilon K_I}{K_D(1+B_P/K_D)^2}\right] B_P. \tag{A9}$$

Since the determinant is always positive, the condition for stability is given by $tr\mathbf{J} < 0$ [43]. By Eq. (A9) this is satisfied when

$$B_P > K_D(\sqrt{\frac{\epsilon K_I K_C}{rK_D}} - 1) = B_I^M\,, \tag{A10}$$

which is the criterion in Eq. (10).

Appendix B: Bacteria-phage-immune model with an infected bacterial class

In this appendix we show that the general results of our model is robust to variations in model formalism. In our model, the time between adsorption of a phage particle to lysis of the bacterial cell, or the latent period, is assumed to be sufficiently small such that the replication and release of new phage particles can be treated as instantaneous. Here we extend the model to account for the latent period by introducing an infected bacterial class F explicitly in which individuals are lysed at a rate η [30]. The generalized model is given by

$$\dot{B} = \overbrace{rB(1-\frac{B+F}{K_C})}^{\text{Growth}} - \overbrace{\phi BP}^{\text{Infection}} - \overbrace{\frac{\epsilon IB}{1+(B+F)/K_D}}^{\text{Immune killing}}\,, \tag{B1}$$

$$\dot{F} = \overbrace{\phi BP}^{\text{Infection}} - \overbrace{\eta F}^{\text{Lysis}} - \overbrace{\frac{\epsilon IF}{1+(B+F)/K_D}}^{\text{Immune killing}}\,, \tag{B2}$$

$$\dot{P} = \overbrace{\beta\eta F}^{\text{Release of phage}} - \overbrace{\phi BP}^{\text{Adsorption}} - \overbrace{\omega P}^{\text{Decay}}\,, \tag{B3}$$

$$\dot{I} = \overbrace{\alpha I(1-\frac{I}{K_I})\frac{B+F}{B+F+K_N}}^{\text{Immune stimulation}} \tag{B4}$$

where F is the population density of the bacteria infected by phage, η is the rate at which the infected bacteria lyse, and the rest of the parameters are defined in the original model in Eqs. (1) – (3).

We simulate this model by fixing $I = K_I$ as in Fig. 5 and show the steady state populations of uninfected bacteria, infected bacteria and phage in Fig. 8. The results show all the same qualitative features as in Fig. 5 including regimes of phage-immune synergism, phage-bacteria-immune coexistence and phage extinction. This indicates that the results of our analysis is robust to the model formulation. The results differ from the model without an infected class only by a scaling of the thresholds $B_P = B_I^S$, $B_P = B_I^M$ and $B_P = B_I^U$. The scaling is caused by a reduction of the effective burst size that results from infected bacteria being killed by the immune response before the phage particles are released. As a result, for the phage infection to successfully produce viral progeny, the lysis must be completed before the bacterial cell is killed by the immune response. Assuming the immune response is at its maximum K_I, this gives the effective burst size at equilibrium

$$\tilde{\beta} = \frac{\eta}{\eta + D(B^* + F^*)}\beta \tag{B5}$$

where the function $D(x) \equiv \frac{\epsilon K_I}{1+x/K_D}$ is the per capita killing rate by the maximum immune response when the total (uninfected and infected) bacteria density is x. B^* and F^* are the equilibrium densities of the uninfected and infected bacteria respectively. Assuming that lysis happens at a sufficiently fast rate compared to the phage infection, the total bacteria density $B^* + F^*$ at equilibrium can be estimated by the equilibrium bacteria density in the limit $\eta \to \infty$, i.e. the equilibrium value for the model without an infected class. The value of $B^* + F^*$ is thus approximated by the value of B_P at each threshold from the original model in Eqs. (1) – (3). This results in the following scaled thresholds:

$$B_P = S(B_I^S)B_I^S\,, \tag{B6}$$

$$B_P = S(B_I^M)B_I^M\,, \tag{B7}$$

$$B_P = S(B_I^U)B_I^U \tag{B8}$$

where the scaling function $S(B) \equiv (1 + D(B)/\eta)$. The scaled thresholds are shown in Fig. 8 and give satisfactory approximation of the transitions between regimes of phage-immune synergism, coexistence and phage extinction. The results of the analysis confirm that the same mechanism for the synergistic effect between phage and immune response applies after accounting for a reduced effective burst size.

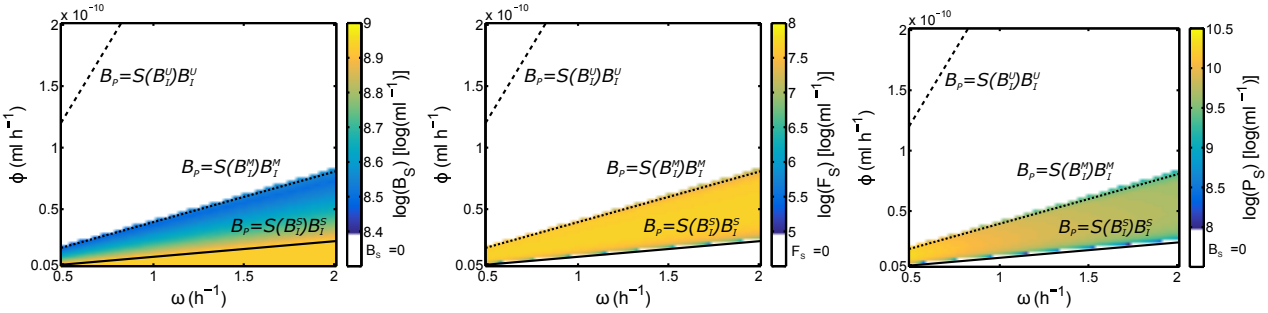

FIG. 8. Heat map showing the dependence of (a) log steady state uninfected bacteria density B_S, (b) log steady state infected bacteria density F_S and (c) log steady state phage density P_S on the phage decay rate ω and adsorption rate ϕ. The solid, dotted and dashed lines are the scaled threshold relations in Eqs. (B6), (B7) and (B8) respectively. The initial conditions are given by $B_0 = B_I^S$, $F_0 = 0$, $P_0 = 10^5$ ml^{-1} and $I_0 = K_I$. The lysis rate $\eta = 2$ h^{-1}.

ACKNOWLEDGMENTS

This work is supported by Army Research Office grant W911NF-14-1-0402. The authors thank Devika Singh for the illustration in Fig. 7.

[1] C. Potera, Environ Health Persp **121**, a48 (2013).
[2] R. M. Carlton, Arch Immunol Ther Exp **47**, 267 (1999).
[3] K. Thiel, Nature Biotechnol **22**, 31 (2004).
[4] J. R. Clark, Future Virol **10**, 449 (2015).
[5] S. Reardon, Nature **510**, 15 (2014).
[6] K. Kingwell, Nat Rev Drug Discov **14**, 515 (2015).
[7] B. François, H. S. Jafri, and M. Bonten, Intensive Care Med , 1 (2016).
[8] S. Hagens and M. J. Loessner, Appl Microbiol Biotechnol **76**, 513 (2007).
[9] S. T. Abedon, Foodborne Pathog Dis **6**, 807 (2009).
[10] B. Leverentz, W. S. Conway, M. J. Camp, W. J. Janisiewicz, T. Abuladze, M. Yang, R. Saftner, and A. Sulakvelidze, Appl Environ Microbiol **69**, 4519 (2003).
[11] S. Guenther, D. Huwyler, S. Richard, and M. J. Loessner, Appl Environ Microbiol **75**, 93 (2009).
[12] J. Seo, D. J. Seo, H. Oh, S. B. Jeon, M.-H. Oh, and C. Choi, Korean J Food Sci An **2** (2016).
[13] C. Loc-Carrillo and S. T. Abedon, Bacteriophage **1**, 111 (2011).
[14] R. J. H. Payne and V. A. A. Jansen, Clin Pharmacol Ther **68**, 225 (2000).
[15] R. J. H. Payne and V. A. A. Jansen, Clinical Pharmacokinetics **42**, 315 (2003).
[16] R. J. H. Payne and V. A. A. Jansen, J Theor Biol **208**, 37 (2001).
[17] B. J. Cairns, A. R. Timms, V. A. A. Jansen, I. F. Connerton, and R. J. H. Payne, PLOS Pathog **5**, 1 (2009).
[18] M. Skurnik, M. Pajunen, and S. Kiljunen, Biotechnol Lett **29**, 995 (2007).
[19] J. Azeredo and I. W. Sutherland, Curr Pharm Biotechnol **9**, 261 (2008).
[20] M. D. Rodney, Trends Microbiol **17**, 66 (2009).
[21] K. L. Timothy and S. K. Michael, Curr Opin Microbiol **14**, 524 (2011).
[22] D. Alemayehu, P. G. Casey, O. McAuliffe, C. M. Guinane, J. G. Martin, F. Shanahan, A. Coffey, R. P. Ross, and C. Hill, mBio **3** (2012), 10.1128/mBio.00029-12, http://mbio.asm.org/content/3/2/e00029-12.full.pdf+html.
[23] D. Gutiérrez, D. Vandenheuvel, B. Martínez, A. Rodríguez, R. Lavigne, and P. García, Appl Environ Microbiol **81**, 3336 (2015), http://aem.asm.org/content/81/10/3336.full.pdf+html.
[24] A. Campbell, Nat Rev Genet **4**, 471 (2003).
[25] J. A. Hermoso, J. L. García, and P. García, Curr Opin Microbiol **10**, 461 (2007).
[26] L. Chao, B. R. Levin, and F. M. Stewart, Ecology **58**, 369 (1977).
[27] B. R. Levin, F. M. Stewart, and L. Chao, Am Nat **111**, 3 (1977).
[28] R. E. Lenski, J Theor Biol **108**, 319 (1984).
[29] J. J. Dennehy, Int J Evol Biol **2012** (2012).
[30] J. S. Weitz, *Quantitative Viral Ecology: Dynamics of Viruses and Their Microbial Hosts* (Princeton University Press, Princeton, New Jersey, 2015).
[31] B. R. Tiwari, S. Kim, M. Rahman, and J. Kim, J Microbiol **49**, 994 (2011).
[32] G. Trigo, T. G. Martins, A. G. Fraga, A. Longatto-Filho, A. G. Castro, J. Azeredo, and J. Pedrosa, PLoS Negl Trop Dis **7**, 1 (2013).
[33] N. B. Pincus, J. D. Reckhow, D. Saleem, M. L. Jammeh, S. K. Datta, and I. A. Myles, PLoS ONE **10**, 1 (2015).
[34] B. R. Levin and J. J. Bull, Am Nat **147**, 881 (1996).
[35] B. R. Levin and J. J. Bull, Nature Rev Microbiol **2**, 166 (2004).
[36] D. M.-Y. Sze, K.-M. Toellner, C. G. de Vinuesa, D. R. Taylor, and I. C. MacLennan, J Exp Med **192**, 813

(2000).
[37] B. Guo, K. Abdelraouf, K. R. Ledesma, K.-T. Chang, M. Nikolaou, and V. H. Tam, Antimicrob Agents Chemother **55**, 4601 (2011).
[38] J. Jubrail, P. Morris, M. A. Bewley, S. Stoneham, S. A. Johnston, S. J. Foster, A. A. Peden, R. C. Read, H. M. Marriott, and D. H. Dockrell, Cell Microbiol **18**, 80 (2016).
[39] T. R. de Kievit and B. H. Iglewski, Infect Immun **68**, 4839 (2000).
[40] K. Sauer, A. K. Camper, G. D. Ehrlich, J. W. Costerton, and D. G. Davies, J Bacteriol **184**, 1140 (2002).
[41] S. L. Gellatly and R. E. W. Hancock, Pathog Dis **67**, 159 (2013).
[42] E. K. Sully, N. Malachowa, B. O. Elmore, S. M. Alexander, J. K. Femling, B. M. Gray, F. R. DeLeo, M. Otto, A. L. Cheung, B. S. Edwards, L. A. Sklar, A. R. Horswill, P. R. Hall, and H. D. Gresham, PLOS Pathog **10**, e1004174 (2014).
[43] S. H. Strogatz, *Nonlinear dynamics and chaos: with applications to physics, biology, chemistry, and engineering* (Westview Press, Boulder, Colorado, 2014).
[44] S. J. Labrie, J. E. Samson, and S. Moineau, Nature Rev Microbiol **8**, 317 (2010).
[45] A. Buckling and P. B. Rainey, Proc R Soc B **269**, 931 (2002).
[46] J. S. Weitz, H. Hartman, and S. A. Levin, Proc Natl Acad Sci U S A **102**, 9535 (2005).
[47] P. Hyman and S. T. Abedon, in *Advances in Applied Microbiology*, Advances in Applied Microbiology, Vol. 70 (Academic Press, 2010) pp. 217–248.
[48] A. R. Hall, P. D. Scanlan, A. D. Morgan, and A. Buckling, Ecol Lett **14**, 635 (2011).
[49] A. Betts, O. Kaltz, and M. E. Hochberg, Proc Natl Acad Sci U S A **111**, 11109 (2014).
[50] A. A. Filippov, K. V. Sergueev, Y. He, X.-Z. Huang, B. T. Gnade, A. J. Mueller, C. M. Fernandez-Prada, and M. P. Nikolich, PLOS ONE **6**, 1 (2011).
[51] K. D. Seed, M. Yen, B. J. Shapiro, I. J. Hilaire, R. C. Charles, J. E. Teng, L. C. Ivers, J. Boncy, J. B. Harris, and A. Camilli, eLife **3**, e03497 (2014).
[52] K. Hodyra-Stefaniak, P. Miernikiewicz, J. Drapała, M. Drab, E. Jończyk-Matysiak, D. Lecion, Z. Kaźmierczak, W. Beta, J. Majewska, M. Harhala, *et al.*, Sci Rep **5**, 14802 (2015).
[53] J. J. Gill and P. Hyman, Curr Pharm Biotechnol **11**, 2 (2010).
[54] M. Khan Mirzaei and A. S. Nilsson, PLOS ONE **10**, 1 (2015).
[55] M. A. Brockhurst and B. Koskella, Trends Ecol Evol **28**, 367 (2013).
[56] Y. Li, A. Karlin, J. D. Loike, and S. C. Silverstein, Proc Natl Acad Sci U S A **99**, 8289 (2002).
[57] G. J. Nau, J. F. L. Richmond, A. Schlesinger, E. G. Jennings, E. S. Lander, and R. A. Young, Proc Natl Acad Sci U S A **99**, 1503 (2002).
[58] A. W. Ensminger, Y. Yassin, A. Miron, and R. R. Isberg, PLOS Pathog **8**, 1 (2012).
[59] R. Capparelli, N. Nocerino, M. Iannaccone, D. Ercolini, M. Parlato, M. Chiara, and D. Iannelli, J Infect Dis **201**, 52 (2010).
[60] M. De Paepe and F. Taddei, PLOS Biol **4**, e193 (2006).
[61] Y. Shao and I.-N. Wang, Genetics **180**, 471 (2008).
[62] A. Handel, E. Margolis, and B. R. Levin, J Theor Biol **256**, 655 (2009).
[63] P. Bhagunde, K.-T. Chang, R. Singh, V. Singh, K. W. Garey, M. Nikolaou, and V. H. Tam, Antimicrob Agents Chemother **54**, 4739 (2010).
[64] J. E. Wigginton and D. Kirschner, J Immunol **166**, 1951 (2001).
[65] A. Wright, C. H. Hawkins, E. E. Anggård, and D. R. Harper, Clin Otolaryngol **34**, 349 (2009).